Journal of Environmental Quality TECHNICAL REPORTS

VADOSE ZONE PROCESSES AND CHEMICAL TRANSPORT

Comparative Mapping of Soil Physical–Chemical and Structural Parameters at Field Scale to Identify Zones of Enhanced Leaching Risk

Trine Norgaard,* Per Moldrup, Preben Olsen, Anders L. Vendelboe, Bo V. Iversen, Mogens H. Greve, Jeanne Kjaer, and Lis W. de Jonge

Preferential flow and particle-facilitated transport through macropores contributes significantly to the transport of strongly sorbing substances such as pesticides and phosphorus. The aim of this study was to perform a field-scale characterization of basic soil physical properties like clay and organic carbon content and investigate whether it was possible to relate these to derived structural parameters such as bulk density and conservative tracer parameters and to actual particle and phosphorus leaching patterns obtained from laboratory leaching experiments. Sixty-five cylindrical soil columns of 20-cm height and 20-cm diameter and bulk soil were sampled from the topsoil in a 15-m × 15-m grid in an agricultural loamy field. Highest clay contents and highest bulk densities were found in the northern part of the field. Leaching experiments with a conservative tracer showed fast 5% tracer arrival times and high tracer recovery percentages from columns sampled from the northern part of the field, and the leached mass of particles and particulate phosphorus was also largest from this area. Strong correlations were obtained between 5% tracer arrival time, tracer recovery, and bulk density, indicating that a few well-aligned and better connected macropores might change the hydraulic conductivity between the macropores and the soil matrix, triggering an onset of preferential flow at lower rain intensities compared with less compacted soil. Overall, a comparison mapping of basic and structural characteristics including soil texture, bulk density, dissolved tracer, particle and phosphorus transport parameters identified the northern one-third of the field as a zone with higher leaching risk. This risk assessment based on parameter mapping from measurements on intact samples was in good agreement with 9 yr of pesticide detections in two horizontal wells and with particle and phosphorus leaching patterns from a distributed, shallow drainage pipe system across the field.

In Denmark, approximately 100 to 150 drinking water wells were closed each year from 1994 to 2001 because of pesticide detections (Geological Survey of Denmark and Greenland, 2009). In the same period, the number of pesticides and pesticide degradation products for which analyses were performed increased. Hence, the increase in pesticide detections should be seen not only as a result of increased use, but also as a result of the increased number of analyses performed. The Danish Pesticide Leaching Assessment Programme (PLAP, http://pesticidvarsling.dk) was initiated in 1998 following the increase in the detection of pesticides and pesticide degradation products. The Programme monitors and evaluates pesticide leaching to drainage water and groundwater to assess leaching risks at field scale. Pesticides included in this program are applied in the prescribed manner to five Danish arable fields at representative locations in Denmark. Detection of pesticides is evaluated in relation to the drinking water quality criterion of 0.1 $\mu g\ L^{-1}$.

The use of hundreds of different compounds with widely contrasting physical and chemical properties in agriculture makes it difficult to generalize about compound transport pathways. However, studies have shown that preferential flow and particle-facilitated transport through macropores significantly contribute to the transport of strongly sorbing pesticides (de Jonge et al., 1998; Villholth et al., 2000; Fox et al., 2004; de Jonge et al., 2004a; Gjettermann et al., 2009; Kjaer et al., 2011). Likewise, studies have shown that macropore transport dominates the particle-facilitated transport of phosphorus (Laubel et al., 1999; de Jonge et al., 2004b; Schelde et al., 2006). There is no absolute definition for macropores based on size. In Jarvis (2007) macropores are defined as pores with diameters larger than 0.3 to 0.5 mm, however, Chen and Wagenet (1992) defines macropores as pores with an equivalent diameter of 0.03 to 5 mm. Pores of this size originate from shrinkage cracks, interaggregate voids, earthworm channels, and roots and are often characterized by relatively high continuity and low tortuosity. Preferential flow through macropores often occurs when the water pressure is close to saturation and at some

J. Environ. Qual. 42:271–283 (2013)
doi:10.2134/jeq2012.0105
Received 8 Mar. 2012.
*Corresponding author (trine.norgaard@agrsci.dk).

T. Norgaard, P. Olsen, A.L. Vendelboe, B.V. Iversen, M.H. Greve, and L.W. de Jonge, Dep. of Agroecology, Faculty of Science and Technology, Aarhus Univ., Blichers Allé 20, P.O. Box 50, DK-8830 Tjele, Denmark. P. Moldrup, Dep. of Biotechnology, Chemistry and Environmental Engineering, Aalborg Univ., Sohngaardsholmsvej 57, DK-9000 Aalborg, Denmark. J. Kjaer, Rambøll, Hannemanns Allé 53, DK-2300 Copenhagen S, Denmark. Assigned to Associate Editor Jim Miller.

Abbreviations: b.g.s., below ground surface; EC, electrical conductivity; NTU, nephelometric turbidity; OC, organic carbon; PLAP, The Danish Pesticide Leaching Assessment Programme; PP, particulate phosphorus; RMSE, root mean square error; TP, total phosphorus; TDP, total dissolved phosphorus.

point exceeds the "water-entry" pressure of the soil. At this point the difference in hydraulic conductivity between the soil matrix and macropores creates a non-equilibrated flow with water flowing rapidly in macropores compared with the wetting front in the matrix (Jarvis, 2007). Macropore transport and preferential flow mainly occur in fractured, clay-rich soil (McCarthy et al., 2002; Jacobsen and Kjaer, 2007), whereas matrix flux dominates in sandy soils (Jarvis et al., 2009).

Surface-applied, otherwise immobile and non-leachable, compounds like phosphorus and some pesticides are sorbed to particles at the soil surface. Because of macropore flow, the compounds bypass much of the adsorption and degradation capacity within the reactive upper soil matrix (Jarvis et al., 2009). Although preferential transport is decisive for the leaching of both weakly sorbing and strongly sorbing chemicals, knowledge is still sparse on how to determine field-scale variability of preferential flow pathways. Direct measurements of soil hydraulic properties are both expensive and time-consuming and often practically impossible (Iversen et al., 2011). However, prediction of preferential transport pathways from easily measured parameters such as soil texture, bulk density, and tracer parameters could provide essential information about field-scale vulnerability in relation to preferential flow paths. Such predictions, nonetheless, require a large coherent data set of both simple soil physical and chemical parameters as well as indicator parameters for preferential flow and transport. de Jonge et al. (2004b) and Poulsen et al. (2006) compared soil physical parameters and bromide transport parameters for 42 columns sampled from the topsoil of an agricultural field in a 20-m × 20-m grid. Both studies compared the distribution of soil physical properties, transport parameters, and leached quantity of colloids and concluded that the most important mechanism controlling colloid leaching is soil structure and related transport parameters. Jarvis et al. (2009) developed a classification scheme to classify the susceptibility of soil to macropore flow in the top- and subsoil horizons and validated this against preferential flow indicators from solute breakthrough curves obtained from other published studies. It was concluded that macropore flow can be predicted reasonably well from easily available soil properties and geographic site information. However, they did not include any field-scale spatial variability in their study. Iversen et al. (2011) developed pedotransfer functions to predict logarithms to the saturated hydraulic conductivity ($\log[K_s]$) and to the unsaturated hydraulic conductivity at a matric potential of −1 kPa $\{\log[k(-1)]\}$ using combinations of different soil physical parameters. From $\log(K_s)$ and $\log[k(-1)]$ they developed a map dividing Denmark into risk categories for macropore flow.

The main objectives of our study were to link basic soil characteristics such as clay content and organic carbon (OC) content to derived soil structural parameters like bulk density, arrival time of the first 5% of the tracer mass, and tracer mass recovery to investigate whether it would be possible to map and predict areas especially vulnerable to leaching at field scale. In this study, phosphorus was used as an example of a strongly sorbing model compound that is prone to be transported by particle-facilitated transport, as also suggested by de Jonge et al. (2004b) and Vendelboe et al. (2011), but phosphorus should not be considered as a surrogate for pesticides. Particle mobilization and transport, solute transport, and particle-facilitated transport of phosphorus were studied at 20-cm × 20-cm cylindrical columns. Finally, on the basis of mapped field distribution of selected leaching parameters, the result of the risk assessment was compared with results from a 9-yr monitoring program for pesticides representing both weakly and strongly sorbing compounds sampled from two horizontal wells located in the northern and southern end of the field at a depth of ~3.5 m.

Materials and Methods

Field Site

The field in Silstrup is located in the northwestern part of Jutland, Denmark (Fig. 1A). The Silstrup field site is located on

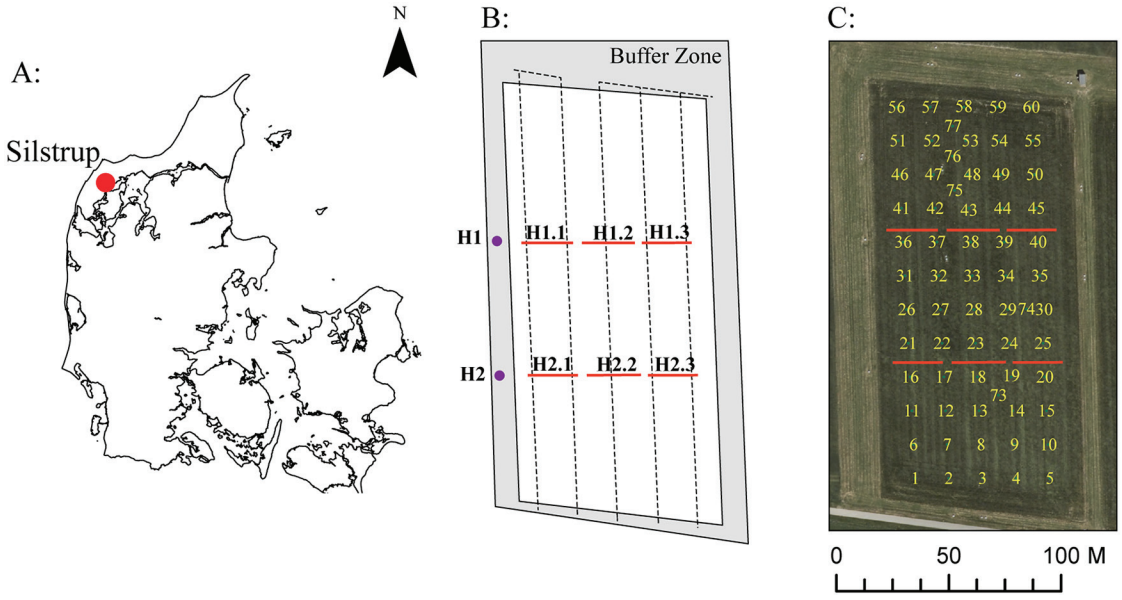

Fig. 1. (A) Location of the field in Silstrup. (B) Sketch showing the two horizontal wells (H1 and H2) separating the field into three parts based on area. H1 and H2 are ~3.5 m below soil surface and each well is separated into three sections (1, 2, and 3). The gray zone illustrates the buffer zone around the field, the dotted lines are tile drains running from south to north inside the field and the purple dots are sampling wells for H1 and H2 (Lindhardt et al., 2001). (C) Sampling grid.

glacial till, a dominant geological formation covering about 43% of all farmland in Denmark (Geological Survey of Denmark and Greenland, 1999; NERI, 2000). The upper meter of the soil is heavily fractured and bioturbated, containing 100 to 1000 biopores m^{-2}. The site's two pedological profiles are classified as Alfic Argiudoll and Typic Hapludoll according to the USDA soil classification system (Lindhardt et al., 2001; Kjaer et al., 2007). The geological setting consists of rather homogenous clay till rich in chalk and chert with local occurrences of thin silt and sand beds (Lindhardt et al., 2001).

The field is a systematically tile-drained loamy field with a cultivated area of 1.69 ha. The tile drains are located at an average depth of 1 m below the ground surface (b.g.s.), and the water table is relatively shallow, located at 1 to 3 m b.g.s (Kjaer et al., 2007). A monitoring well is established at the outlet of the drainage system for collection of drainage water by continuous flow-proportional sampling. Furthermore, the field is equipped with two horizontal wells (H1 and H2, Fig. 1B) drilled perpendicular to the edge of the field separating it into three equal-sized sections. The two wells are approximately 3.5 m b.g.s and each well consists of three 18-m screen sections separated by 1-m bentonite seals. The sections are named 1, 2, and 3, and thus the sections in H1 are identified as H1.1, H1.2, and H1.3. Pesticide analyses are performed on water samples from section 2 in H1 and H2 every month, whereas water from sections 1 and 3 is analyzed three times a year (Lindhardt et al., 2001). Geological properties, soil hydrology, and monitoring equipment are further described in Lindhardt et al. (2001) and Kjaer et al. (2007).

Before sampling, the Silstrup field had not been tilled for almost 2 yr. A thorough overview of management practice performed on the field in Silstrup from 2006 to 2010 can be found in Table 1. The field was plowed in December 2008 to 23 cm depth and harrowed twice to 5 cm depth in March 2009. Since then, soil settling was only disturbed when injecting slurry to 10 cm soil depth in April 2009 and to 4 to 5 cm soil depth in September 2009.

Sampling

Sixty-five cylindrical 20-cm × 20-cm soil columns were sampled from the topsoil on 10 Oct. 2010. The columns were sampled from a rectangular 15-m × 15-m grid (Fig. 1C). To avoid recurring phenomena caused by field cultivation, sampling points were randomly placed either at the grid intersects or 1 m away from the grid intersects in random directions. The columns were pushed into the soil by a hydraulic press mounted on a tractor until the edge of the column was level with the soil surface. Then the columns were carefully excavated by hand, trimmed at the bottom, and sealed. The sampling holes were carefully filled after sampling with soil from the neighboring field. At the time of sampling the field was cultivated with red fescue (*Festuca rubra* L.). The columns were stored at 2°C until further treatment in the laboratory. Adjacent to the column sampling points, bulk soil was sampled from the same 20 cm soil depth.

Physical and Chemical Soil Properties

Bulk density was determined from weights of the columns after drying at 105°C. Texture of the bulk soil samples was determined according to Gee and Or (2002) by a combined sieve/hydrometer method. Organic carbon was determined on a LECO analyzer coupled with an infrared CO_2 detector (Thermo Fisher Scientific Inc.). Interpolated maps for comparative mapping of soil physical, chemical and structural parameters were obtained from ordinary kriging in ArcMap 10.0. The pH was measured in a soil/water solution of 1:4 by volume and electrical conductivity (EC) was measured in a soil/water solution of 1:9 by volume for all 65 bulk soil samples.

Applying the Dexter et al. (2008) "Clay Saturation" Concept

According to Dexter et al. (2008) the ability of soils to maintain or regenerate functional structure, soil–water repellency, satisfactory tilth conditions, and clay dispersion can be related to the ratio between clay and OC, termed the Dexter threshold ratio *n*. Dexter et al. (2008) showed that the optimal ratio, *n*, between clay and OC is 8 to 11 with 10 being the most optimal ratio. At this ratio a complex is formed by the association of one unit mass of OC with 10 g clay. Below this threshold ratio, the soil is saturated with OC. Saturated soils, with $n < 10$ and <10 g of clay per unit of mass OC, have improved soil physical properties compared with OC-depleted soils ($n > 10$). In soils where $n > 10$, the pool of non-complexed clay contributes to the pool of readily dispersible clay colloids that may be transported by macropores to the aquatic environments (Dexter et al., 2008; de Jonge et al., 2009).

Column Leaching

Immediately after sampling, air permeability, and air-connected porosity were measured on the columns. Leaching experiments were performed within 4 to 20 wk from sampling. Before leaching, each column was saturated from the bottom in artificial soil water (0.652 mM NaCl, 0.025 mM KCl, 1.842 mM $CaCl_2$, and 0.255 mM $MgCl_2$; pH = 6.38; EC = 0.6 mS cm^{-1}) for approximately 3 d and then drained to −20 cm matric potential relative to the center of the column during a period of ~3 d.

For the leaching experiment, each column was placed on a 1-mm steel mesh, and water was applied from a rotating irrigation

Table 1. Management practice applied to the field in Silstrup from 2006 to 2010. Dates of fertilizer and pesticide application are not included in the table. Neither is harvest of winter wheat and spring barley, which negligibly disturbs the soil.

Management practice	Date
Pig slurry, surface applied	26 Apr. 2006
Plowed, 22-cm depth	20 Sept. 2006
Sowing winter wheat	22 Sept. 2006
Stubble harrowed, 5-cm depth	29 Aug. 2007
Plowed, 27-cm depth	11 Dec. 2007
Harrowed, 5-cm depth	21 Apr. 2008
Leveled and rolled	22 Apr. 2008
Harrowed, 10-cm depth	5 May 2008
Sowing fodder beet	7 May 2008
Harvest of fodder beet	27 Oct. 2008
Plowed, 23-cm depth	15 Dec. 2008
Harrowed twice, 5-cm depth	30 Mar. 2009
Pig slurry application, 10-cm soil depth	2 Apr. 2009
Rolled	11 Apr. 2009
Sowing spring barley	11 Apr. 2009
Pig slurry application, 4–5-cm soil depth	15 Sept. 2009

head with 44 needles placed randomly to ensure homogenous application on the column surface. There was free drainage from the bottom of the columns. Effluent for further analyses was collected through a funnel in plastic bottles placed on a rotating disc below the column setup. The columns were irrigated with artificial rainwater (0.012 mM $CaCl_2$, 0.015 mM $MgCl_2$, and 0.121 mM NaCl; EC = 0.025 mS cm^{-1}; pH = 5.76–7.26) with an intensity of 10 mm h^{-1}. A 1-h rainstorm of this intensity occurs at a frequency of once annually in Denmark (Arnbjerg-Nielsen et al., 2006). The time taken for the first drop of water to exit the column was recorded and defined as water breakthrough time. Water breakthrough time was registered after 12 to 40 min meaning that the fastest first drop from a column occurred after 12 min and the latest after 40 min, and from the time of breakthrough the columns were irrigated for 6.5 h. Tritium was used as a conservative tracer and applied as a pulse for 10 min when water outflow was steady (time = 0). Steady outflow was defined as the point when the column outflow volume became constant over time. Outflow from the columns was generally stable 20 min after breakthrough with a few exceptions. The irrigation rate when applying the tritium tracer was 10 mm h^{-1} as well.

Effluent was collected for 6.5 h and analyzed for turbidity, pH, EC, total phosphorus (TP), total dissolved phosphorus (TDP), and tritium activity. Turbidity, pH, and EC were measured on water from all sampling intervals separately, but to minimize the number of samples for TP and TDP analyses, water samples were pooled after the first three sampling intervals (i.e., after 30 min).

Turbidity was measured on a Hach 2100AN turbidimeter (Hach, Loveland, CO) equipped with an EPA filter, measuring at wavelengths from 400 to 600 nm. The nephelometric turbidity (NTU) is assumed proportional to particle concentration (mg L^{-1}). The correlation between NTU and particle concentration was obtained from turbidity measurements on different soil suspensions. The different suspensions were made from a main suspension obtained by dispersing bulk soil from Silstrup in deionized water and isolating particles <2 μm by gravitational sedimentation. Two relationships (one power and one linear) were used to calculate the particle concentration (Fig. 2):

$$\text{For NTU} < 1000: C = 1.75 \times NTU^{0.855} \quad [1]$$

$$\text{For NTU} > 1000: C = 0.376 \times NTU + 272.44 \quad [2]$$

Total dissolved P was defined as the phosphorus concentration present in the supernatant after centrifuging for 1 h at 5000 G (lower cut-off particle diameter of 0.1 μm). Phosphorus concentrations were determined using acid persulfate digestion in an autoclave (120°C, 200 kPa, 30 min) (Koroleff, 1983) followed by a colorimetric technique (Murphy and Riley, 1962). The fraction of particulate phosphorus (PP) was estimated as the difference between TP and TDP.

Tritium decay per minute was determined on each effluent sample throughout the experiment on a liquid scintillation analyzer (Tri-Carb 2250 CA).

Results and Discussion

Physical and Chemical Soil Properties

Clay content in the topsoil across the field were from 0.14 to 0.19 kg kg^{-1} and OC was from 0.017 to 0.022 kg kg^{-1} (Table 2). Highest clay contents and lowest OC contents were found in the

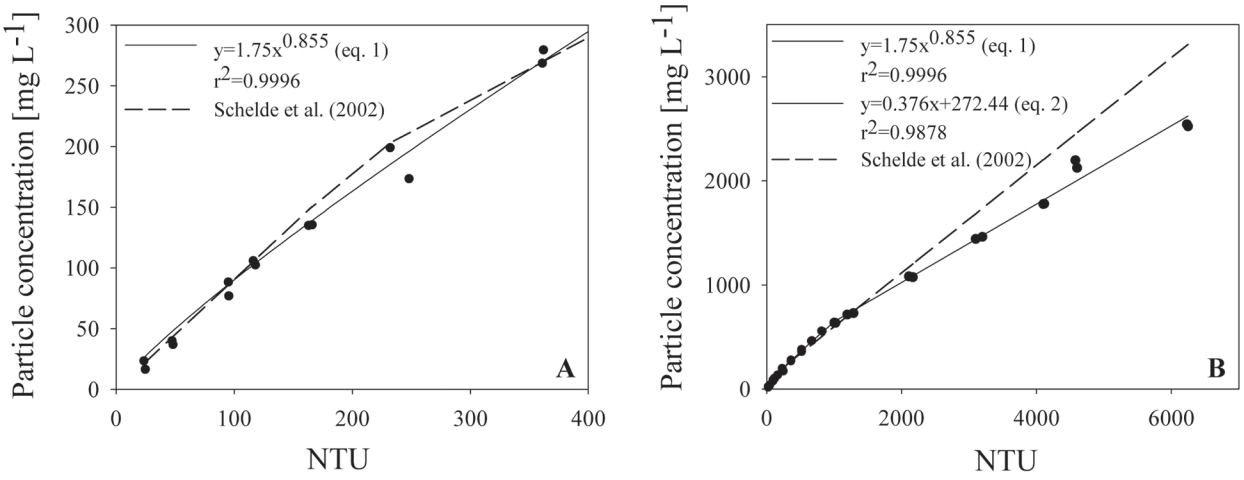

Fig. 2. A linear and a power correlation describe the correlation between nephelometric turbidity (NTU) and particle concentration. (A) A close-up of the 0 to 400 NTU section of the scale; (B) the entire range. A correlation from Schelde et al. (2002) is shown with the dashed line. Schelde et al. (2002) used two linear relationships—one for NTU < 200 and another for NTU > 200.

Table 2. Minimum, maximum, and mean contents of measured soil characteristics.

	Clay content (<2 μm)†	Silt content (2–50 μm)†	OC content†‡	Bulk density§	pH†	EC†‡
	kg kg^{-1}	kg kg^{-1}	kg kg^{-1}	g cm^{-3}	–	mS cm^{-1}
Min. value	0.14	0.23	0.017	1.39	6.39	0.40
Max. value	0.19	0.33	0.022	1.60	7.49	0.71
Mean	0.16	0.30	0.020	1.50	6.75	0.47

† Determined on bulk soil samples taken adjacent to each soil column.

‡ EC, electrical conductivity; OC, organic carbon.

§ Determined from dry weights of the columns.

northern part of the field. Thus, clay and OC gradients run in opposite directions (Fig. 3A and B). Interpolation was done in geostatistical analyst in ArcMap 10.0. Omni-directional global variograms were calculated and different theoretical models were fitted based on root mean square error (RMSE). Information about interpolation models and semivariograms is given in Table 3.

Three Dexter et al. (2008) saturation lines representing n = 8, 10, and 11 are included in the plot in Fig. 4. Considering the line representing n = 10, the clay at all sampling points, except for three located in the northern part of the field, should be OC-saturated. Therefore, according to the Dexter et al. (2008) concept the soil should be stable and able to regenerate from external physical disturbance (de Jonge et al., 2009). In Fig. 3C it is possible to draw a line where, roughly, the upper 40% of the field represents an area with higher Dexter n ratios. Assuming that a soil is OC depleted if n > 8.5, this northern part of the field is not saturated with OC. The Dexter map in Fig. 3C is not interpolated from single-point clay/OC ratios at each point, but complied by making the ratio of the clay and OC grids, and therefore there are no semivariogram for this map in Table 3.

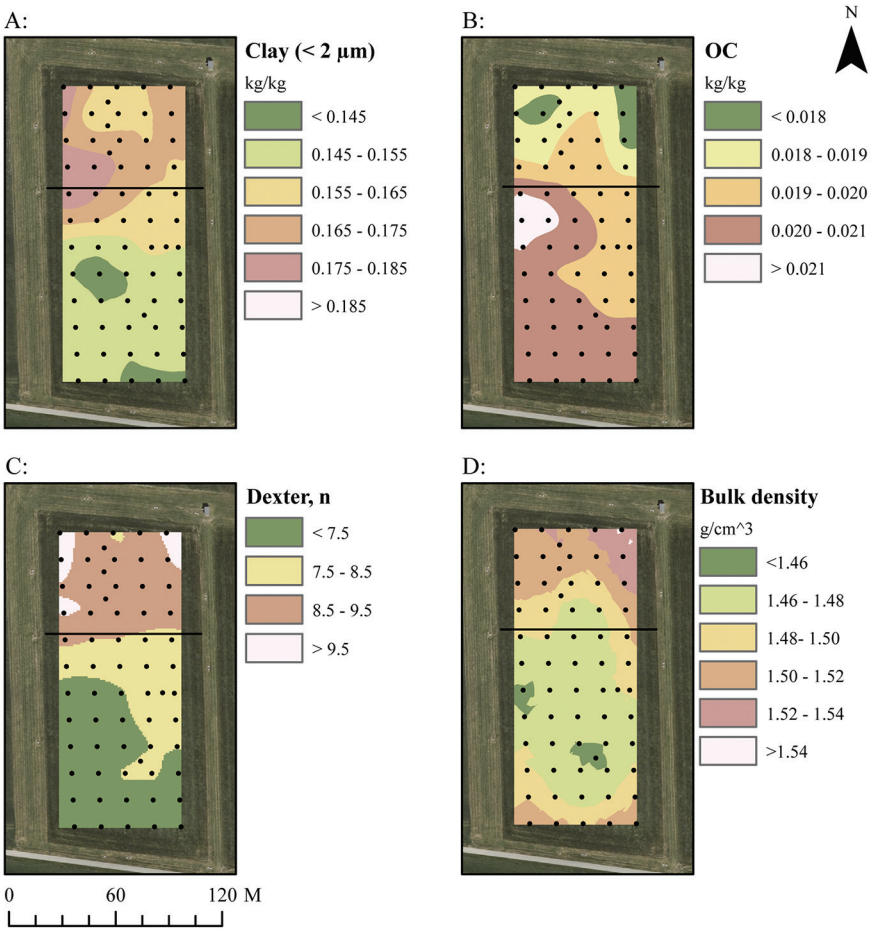

Fig. 3. Contour maps of (A) clay content, (B) organic carbon (OC) content, (C) Dexter's ratio, *n*, and (D) bulk density across the field in Silstrup. The black intersecting lines on all four maps are added to emphasize the upper one-third of the field.

Similar to clay content, bulk density was between 1.39 and 1.60 g cm^{-3} (Table 2 and Fig. 3D), and the highest values were found in the northern part of the field. Together with soil management, the ratio between clay and OC, expressed by Dexter's n, can be a controlling factor for field-scale variations in bulk density. Keller and Hakansson (2010) developed model equations for estimation of bulk density from the soil particle size distribution and soil organic matter content and found that bulk density especially was controlled by organic matter content. Higher bulk densities in the northern part of the field may lead to a more compact, less permeable soil matrix with a decreased volumetric content of macropores that are well aligned and well connected.

Variations in air permeability and air-connected porosity in situ, measured right after the columns where sampled, are shown in Fig. 5A and B. Both air-phase parameters increased toward a hot-spot area of high air-connected porosity and air permeability in the southeastern part of the field where the lowest dry bulk densities are also located (Fig. 3D). In general, variations in air-connected porosity and air permeability agreed well.

Water content of the columns at the time of sampling was between 0.30 and 0.35 cm^3 cm^{-3} and thus, there is no clear variation in topography because of water content across the field.

Table 3. Partial sill, nugget, major range, kriging interpolation model, root mean square error (RMSE), and nugget/sill ratio for the semivariograms obtained from each interpolated map. All interpolations were carried out in ESRI ArcMap 10.0. The interpolated Dexter map was found from raster calculations of the organic carbon and clay raster grids.

	Partial sill	Nugget	Major range	Model	RMSE	Nugget/sill ratio
Bulk density	9.73×10^{-4}	1.70×10^{-3}	120	Exponential	4.63×10^{-2}	1.75
Clay	1.95×10^{-4}	3.67×10^{-5}	160	Exponential	6.67×10^{-3}	0.19
OC	1.17×10^{-6}	3.71×10^{-7}	120	Exponential	7.35×10^{-4}	0.32
5% arrival time	2.71×10^{-2}	0.118	140	Exponential	0.37	4.36
Tritium recovery	36	122	120	Spherical	11.9	3.34
Acc. particle mass	585	1024	107	Exponential	37.6	1.75
Acc. PP mass†	1.41×10^{-2}	5.12×10^{-2}	160	Circular	0.24	3.64
Air permeability	223	250	23	Circular	23	1.12
Air-connected porosity	1.33×10^{-4}	3.60×10^{-4}	160	Exponential	2.21×10^{-2}	2.70

† PP, particulate phosphorus.

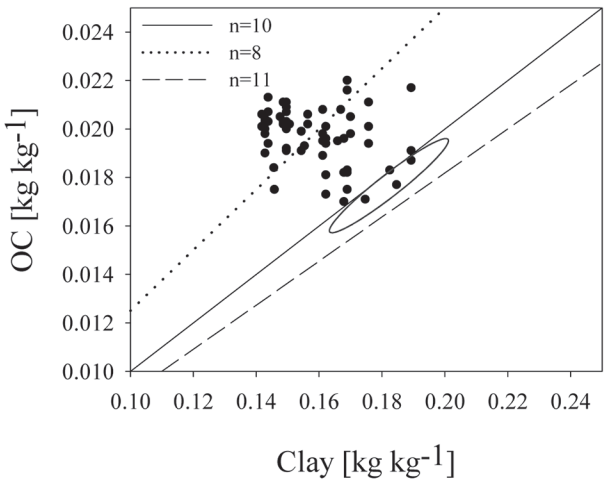

Fig. 4. Organic carbon content (OC) as a function of clay content in the field in Silstrup. Clay/OC ratios representing *n* = 8, 10, and 11 are shown. The three OC-depleted points, evaluated according to *n* > 10 (sampling points 51, 56, and 60), have been circled on the figure.

Tritium Breakthrough Curves

Tritium was applied at steady water outflow (generally after 20 min, denoted as time = 0). The curves are arranged according to increasing bulk densities (Fig. 6). Within the 6.5 h of leaching, in general 0.83 to 1.17 pore volumes passed the columns. With a few exceptions, the breakthrough curves peak after only a small quantity of the pore volume has passed, indicating strong preferential flow pathways. As bulk density increases, toward the lower right plot in Fig. 6, the relative tracer concentration peaks increase and at the same time the curves become increasingly skewed to the right. These higher peak concentrations might originate from well-aligned and well-connected macropores, and the asymmetric and right-skewed form of the breakthrough curves also indicates a highly heterogeneous soil where the transport pathways are dominated by macropore flow. Nevertheless, the pronounced tailing on some of the curves suggests that a small fraction of solute was limited by diffusion between the mobile and immobile water phase (Kjaergaard et al., 2004). Similarly, Kjaergaard et al. (2004) observed asymmetric breakthrough curves for soil with clay contents above 18% and Glaesner et al. (2011) reported earlier breakthrough for loamy soils than for sandy loams.

Tritium mass recovery was on average 67%. A contour map of tritium mass recovery percentages is shown in Fig. 7A; the highest recoveries were found within the northern one third of the field. Glaesner et al. (2011) found an average mass recovery of 94% after approximately 10 h of leaching with a suction of −50 cm applied at the bottom of the columns. The larger amount of tritium recovered in their study was probably caused by the longer sampling time compared with the 6.5 h of sampling in our experiments.

The 5% tritium arrival time is defined as the time when 5% of the applied tritium has been detected in the effluent, and this parameter was found from mass-accumulated tritium curves. Figure 7B shows field-scale variations in 5% arrival time; the lowest values were found to the north. Nonparametric shape measures for solute breakthrough curves were evaluated in Koestel et al. (2011) based on a dataset of 115 tracer breakthrough curves from the literature. In their study they identify the relative arrival time of the first 5% of the tracer mass as the most robust shape parameter to serve as an indicator for preferential flow and transport. In Silstrup high tritium recovery percentages were obtained at fast 5% tritium arrival times and thus fast breakthrough. This negative correlation confirms that short retention times in the compacted columns with pronounced macropore flow result in higher recoveries of tritium in the effluent because of the limited solute exchange with the inner, immobile soil matrix.

Particle Leaching

The conversion from NTU to particle concentration in Fig. 2 found by Schelde et al. (2002) uses two linear relationships. Although these linear relations cover up to 200 NTU for the soil in Silstrup relatively well, they overestimate concentrations exceeding 200 NTU. Clay and OC contents from the soil used in Schelde et al. (2002) were 0.16 and 0.015 kg kg^{-1}, respectively, and although these contents are similar to the soil in Silstrup, specific conversions for each soil are needed to calculate correct particle concentrations.

Particle leaching curves for all 65 columns are shown in Fig. 8. The particle concentration associated with water breakthrough (first flush, here defined at 2.4 mm outflow) was high compared to the stable particle concentration reached after ~10 mm outflow. This particle leaching dynamic was also found by Schelde et al. (2002) and Vendelboe et al. (2011), among others, in similar leaching experiments on undisturbed soil columns. During first flush, loose particles at the macropore walls are detached by the irrigating water and transported to the collecting bottles at the bottom of the soil columns (de Jonge et al., 2004b; Majdalani et al., 2008; Vendelboe et al., 2011). Particle concentrations during first flush varied between 62 and 390 mg L^{-1} with a mean value of 177 mg L^{-1}. Peaks on the particle concentration curves after first flush were ascribed to the clogging

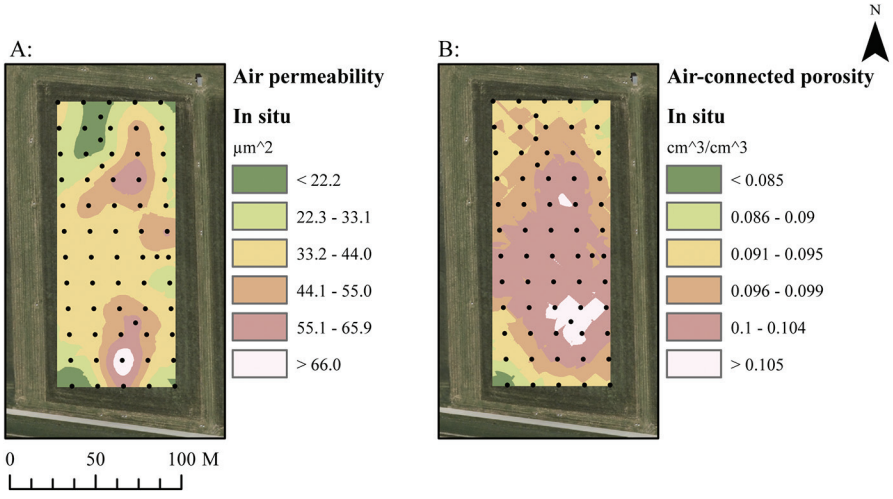

Fig. 5. Variations in (A) air permeability (µm^2) and (B) air-connected porosity (cm^3 cm^{-3}) across the field.

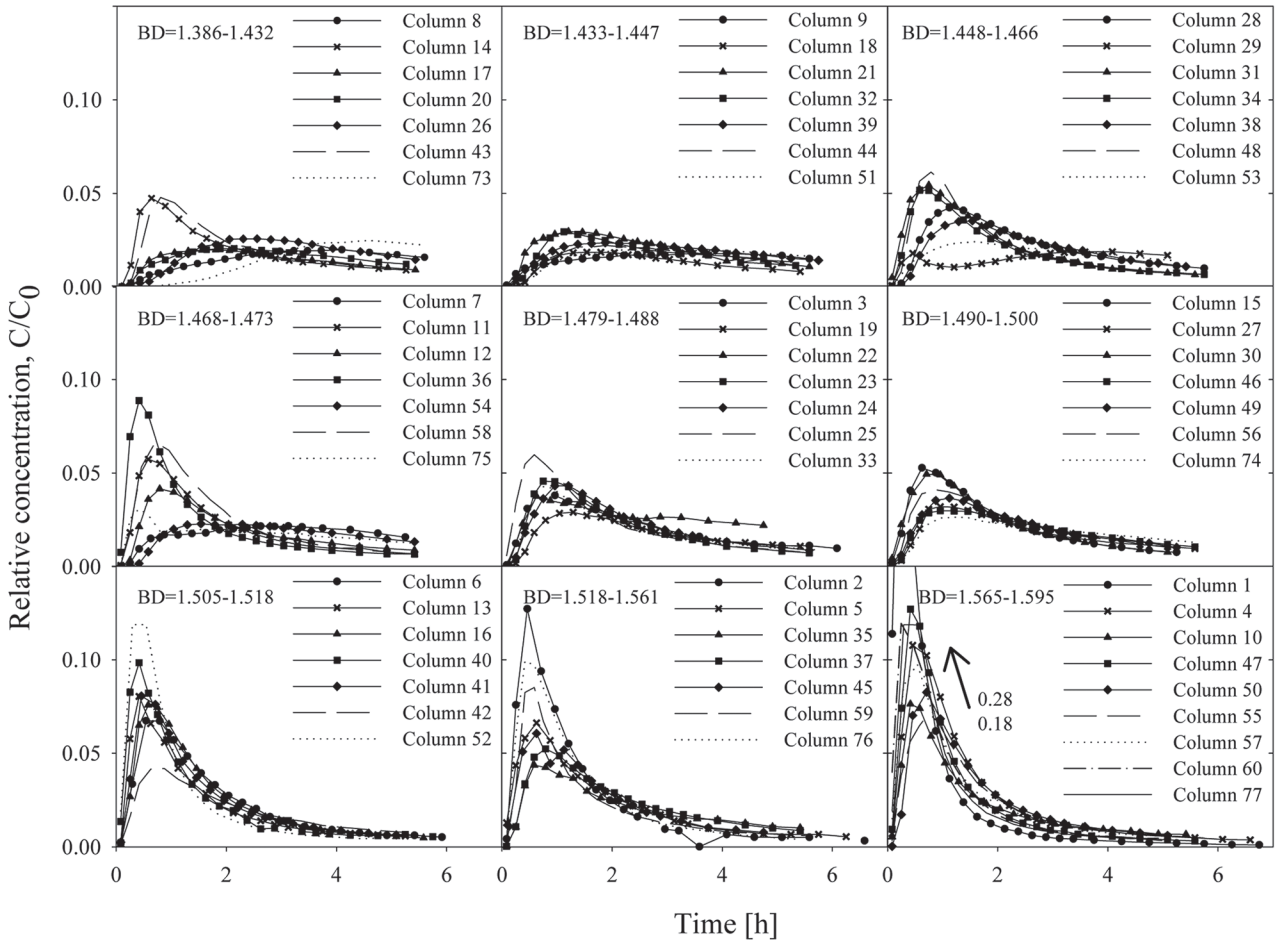

Fig. 6. Tritium breakthrough curves from the leaching experiments for increasing bulk densities. Note: For column 1 (bottom right) there are two points (0.28 and 0.18) that are above the scale.

and unclogging of individual pores leading to a water pressure build-up in one or more blocked macropores (de Jonge et al., 2004b; Vendelboe et al., 2011).

Because of the significant correlation of bulk density with the total accumulated mass of particles leached (r = 0.29) shown in Table 4, the particle leaching curves in Fig. 8 have been arranged according to increasing bulk densities. However, it was not possible to see any clear trends in the shape or change in the particle leaching curves as bulk density increases in the figure.

Water breakthrough time from the columns varied between 12 and 40 min corresponding to macropore velocities between 0.29 and 0.95 m h^{-1}, calculated as the soil column height divided by the water breakthrough time. In similar leaching studies, Schelde et al. (2002) and de Jonge et al. (2004b) obtained macropore velocities ranging between 0.30 and 2.4 m h^{-1} and 0.11 and 0.82 m h^{-1}, respectively. These similar leaching experiments were all performed on undisturbed soil columns sampled from sandy loam soils in Denmark. The higher macropore flow velocities obtained by Schelde et al. (2002) might be caused by the higher irrigation intensities of 11 to 30 mm h^{-1}, while de Jonge et al. (2004b) used the irrigation intensity of 10 mm h^{-1} also used in this study.

After 50 min of irrigation the high particle concentrations, mainly associated with first flush, reached a lower and more constant level for all columns (Fig. 8). Table 5 shows first-flush leached particle concentrations from this and similar laboratory studies, all on undisturbed columns. Even though the particle

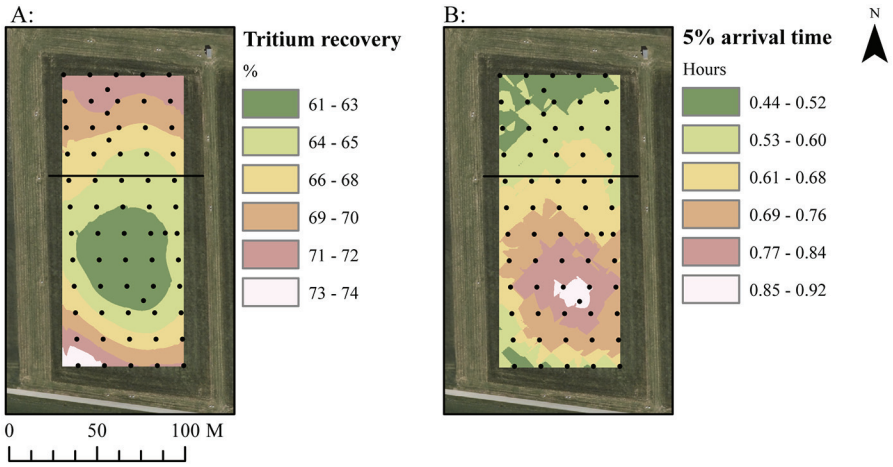

Fig. 7. Contour maps showing tritium recovery and 5% arrival time. The black intersecting lines on the two maps are added to emphasize the upper one-third of the field.

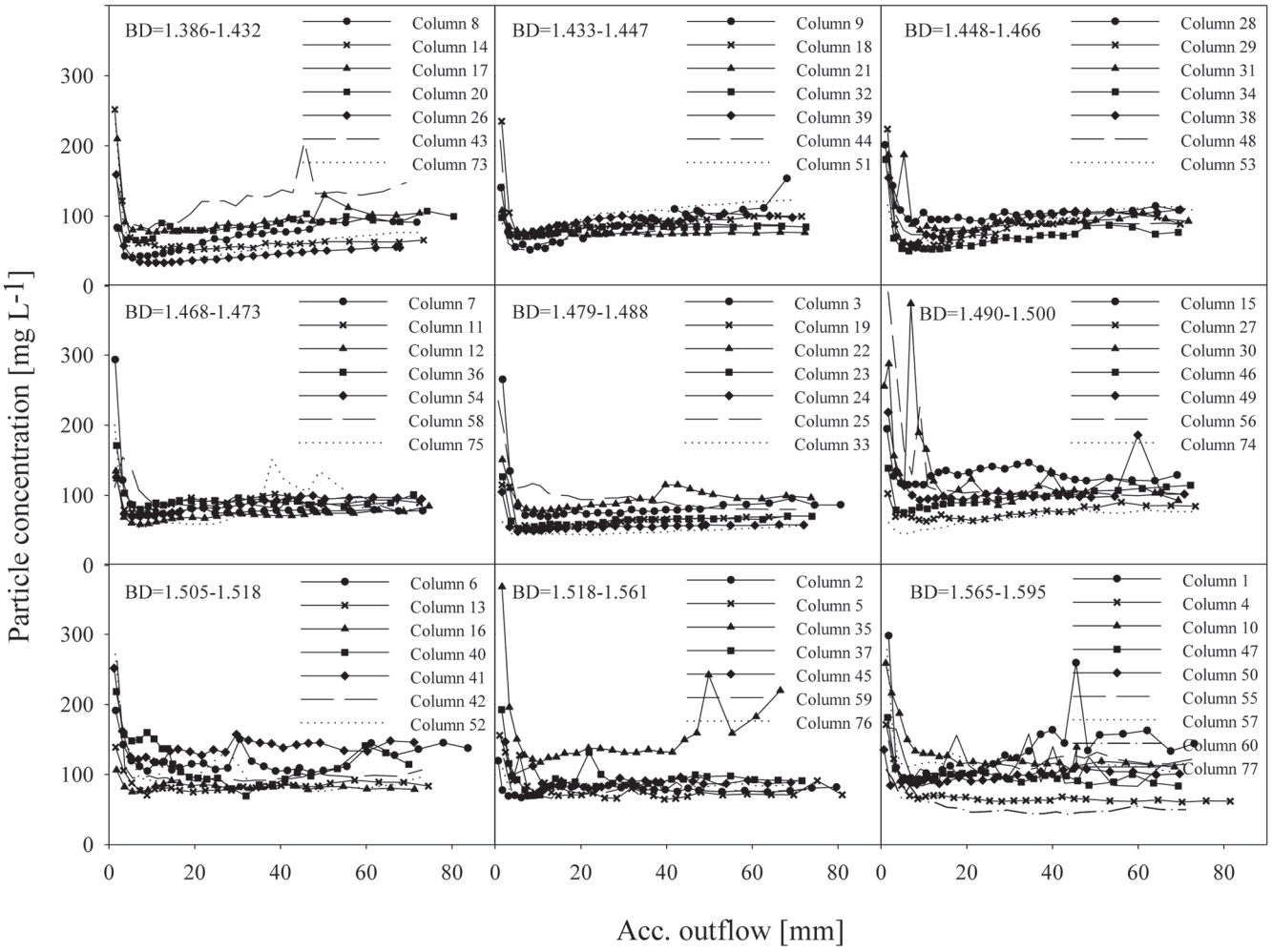

Fig. 8. Particle concentrations in the effluent as a function of accumulated outflow. The curves are in the order of increasing bulk densities.

Table 4. Pearson correlation coefficient, *r*.

	Clay	OC†	Dexter, *n*	Bulk density	Total accumulated particle mass‡	First-flush particle mass§	Total accumulated PP mass†¶	First-flush PP mass#	Tritium recovery	5% arrival time
	— kg kg^{-1} —		–	g kg^{-1}	——————— mg ———————				%	h
Clay (kg kg^{-1})	1.00	−0.24*	0.85***	0.13	0.24	0.01	0.09	−0.01	0.06	−0.15
OC (kg kg^{-1})	–	1.00	−0.71***	−0.46***	−0.12	0.10	−0.14	0.06	−0.19	0.20
Dexter, *n*	–	–	1.00	0.35**	0.23	−0.05	0.14	−0.04	0.15	−0.21
Bulk density (g kg^{-1})	–	–	–	1.00	0.29*	0.17	−0.08	0.15	0.72***	−0.68***
Total acc. particle mass (mg)	–	–	–	–	1.00	0.66***	0.19	0.27*	0.20	−0.32*
First-flush particle mass (mg)	–	–	–	–	–	1.00	0.05	0.66***	0.09	−0.17
Total acc. PP mass (mg)	–	–	–	–	–	–	1.00	0.35**	−0.11	0.08
First-flush PP (mg)	–	–	–	–	–	–	–	1.00	0.16	−0.17
Tritium recovery (%)	–	–	–	–	–	–	–	–	1.00	−0.74***
5% arrival time (h)	–	–	–	–	–	–	–	–	–	1.00

*$P < 0.05$.

**$P < 0.01$.

***$P < 0.001$.

† OC, organic carbon; PP, particulate phosphorus.

‡ Total accumulated particle mass leached at 60 mm outflow.

§ First-flush particle mass leached at 2.4 mm outflow.

¶ Total accumulated PP mass leached at 60 mm outflow.

First-flush PP mass leached at 2.4 mm outflow.

Table 5. Literature values for particle concentrations leached with first flush. All literature values are from irrigation experiments on undisturbed soil columns.

Reference	Min.	Max.	Average	Clay content	Irrigation rate	Duration
	mg L^{-1}			kg kg^{-1}	mm h^{-1}	h
Silstrup, 2010	62	390	177	0.14–0.19	10	6.5
de Jonge et al. (2004b)	188	1849	448	0.11–0.16	10	3.5
Vendelboe et al. (2011)	124	369	235	0.11–0.23	10	4
Schelde et al. (2002)	80	4100	–	0.157 (avg.)	11–30	2–5
Kjaergaard et al. (2004)	6	167	–	0.12–0.43	1	6

concentrations associated with first flush in our study were high compared with subsequent concentrations, they were low compared with other similar leaching studies, except for Kjaergaard et al. (2004), who found smaller first-flush values. Their columns were, however, also sampled from a no-till system, the applied irrigation rate was considerably lower than the one we used and a lower boundary of −5 cm was applied to the columns during the leaching experiment. The no-till management conditions imposed on the field in Silstrup might result in lower leached particle concentrations because the immediate particle release or soil dispersibility depends on particle mobilization and consequently soil tillage (Etana et al., 2009). Thus, Gjettermann et al. (2009) found average leached particle concentrations in the effluent ranging from 50 to 97 mg L^{-1} and 183 to 295 mg L^{-1} for columns sampled from minimally disturbed and plowed sandy loam soils, respectively.

The range of particle concentrations in first flush from our undisturbed soil columns (62–390 mg L^{-1}) were compared with those found in other field-scale studies. Laubel et al. (1999) performed six rain simulations on two 25-m^2 plots on loamy soil (clay content: 15.5–22.0%). The irrigation intensities varied between 15.3 and 37.0 mm over 2 to 3 h. Water samples were collected manually from the drainpipe outlet and particulate matter concentrations during first flush varied between 63 and 334 mg L^{-1}. Grant et al. (1996) measured particulate matter concentrations in the main outlet of a drainage network in a 13.3 ha intensively farmed catchment area of mainly sandy loam soil. The concentration peaked during a rainstorm event on 14 Sept. 1993 at 165 mg L^{-1}. El-Farhan et al. (2000) obtained peak colloid concentrations of up to 265 mg L^{-1} after repeated in situ infiltration experiments at field scale. In situ field experiments by Villholth et al. (2000) and Schelde et al. (2006) also showed high particle concentrations after breakthrough followed by a decrease to a constant level.

Particulate Phosphorus Leaching

The shape of TP and PP concentration curves was similar to the shape of the particle leaching curves with high first-flush concentrations that stabilized after approximately 10 mm outflow (curves not shown). Particulate P concentrations varied between 0.07 and 1.73 mg L^{-1} during first flush and reached a constant level between 0.1 and 0.35 mg L^{-1}. Figure 9A shows the PP concentrations against particle concentrations in the first three sampling intervals (i.e., the first 3 × 10 min) for each column, and as in similar leaching studies by Laubel et al. (1999), Schelde et al. (2006) and Vendelboe et al. (2011), there is a linear correlation between particle and PP concentrations. A linear correlation was likewise obtained between the first-flush particle mass and the first-flush PP mass (Fig. 9B).

On a weekly basis, particle concentrations, TP concentrations and TDP concentrations were measured on pooled samples of drainage water from the flow-proportional sampling in Silstrup. Measured particle and PP concentrations in drainage water samples from 7 Oct. 2010, to 13 Apr. 2011, are shown in Fig. 10A together with daily precipitation rates. PP concentrations are calculated as the difference between TP and TDP concentrations. After notable rain events, both particle and PP concentrations peak as a result of first flush. The particle peak concentrations were, however, much lower than those obtained within first flush on the columns, and because of lower particle concentrations we also get lower PP concentrations. This difference is probably caused by dilution when pooling the samples of drainage water and it is therefore difficult to compare concentration levels.

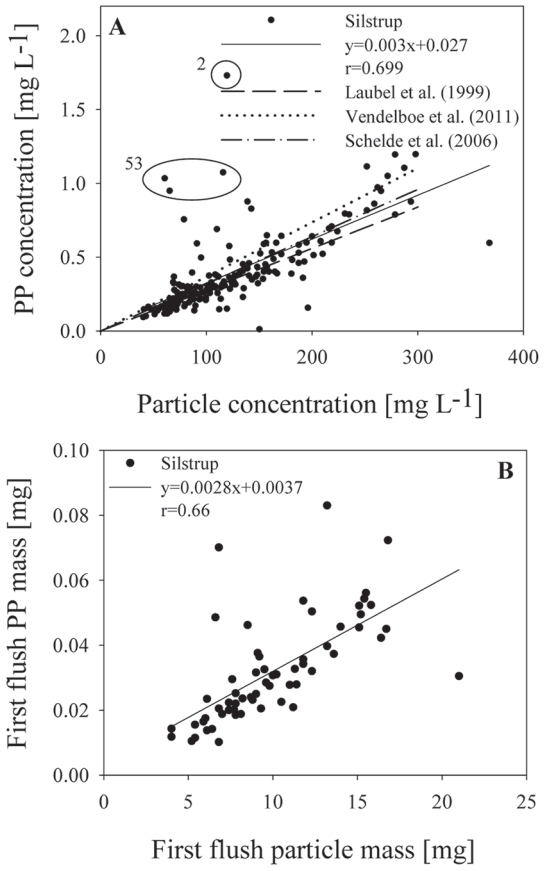

Fig. 9. (A) Particulate phosphorus (PP) concentrations as a function of particle concentrations, and three linear regressions from the literature. Laubel et al. (1999): $y = 0.0028x$, Schelde et al. (2006): $y = 0.0032x$, and Vendelboe et al. (2011): $y = 0.00368x + 7.02 \times 10^{-5}$. Note: data from column 53 and the first data point of column 2 have been circled because they differ from the rest of the columns. Without these points the regression line would be: $y = 0.0031x - 0.0117$, $r = 0.838$. (B) First-flush PP mass as a function of first-flush particle mass.

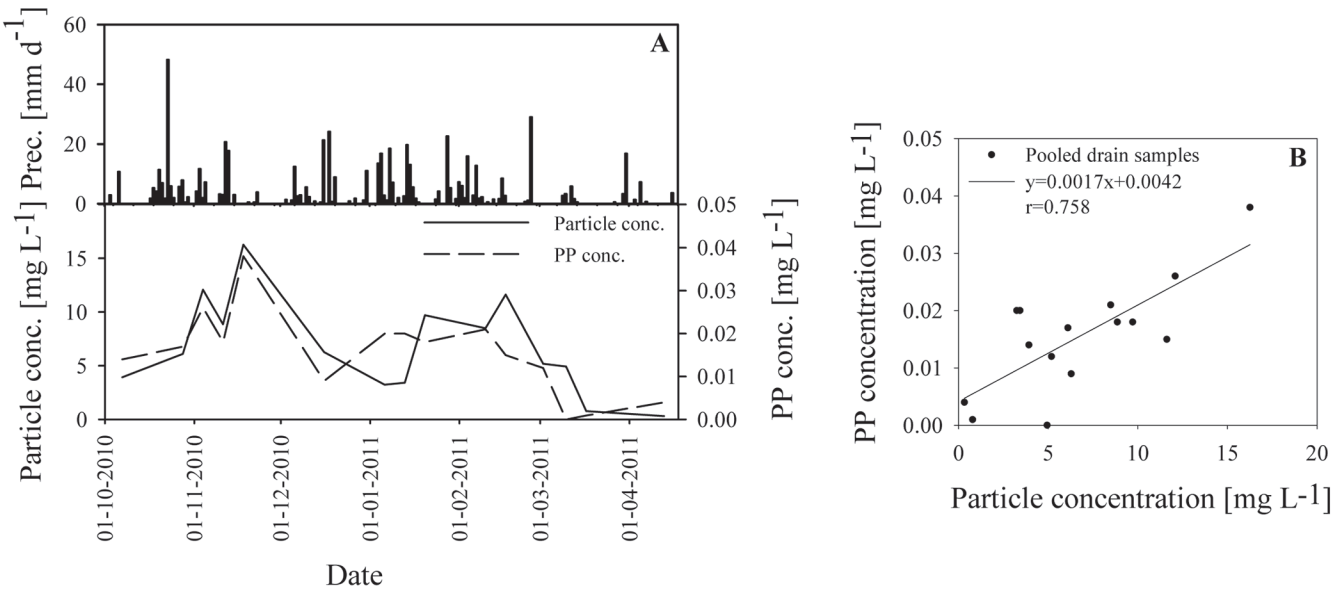

Fig. 10. (A) Precipitation (mm d^{-1}), particle concentrations (mg L^{-1}), and particulate phosphorus (PP) concentrations (mg L^{-1}) from weekly pooled drain water sampled from 7 Oct. 2010 to 13 Apr. 2011. (B) Particulate phosphorus concentrations as a function of particle concentrations in weekly pooled samples from the drainage system in Silstrup. The samples are from 7 Oct. 2010 to 13 Apr. 2011.

However, the tendencies are the same as found in the columns and also Fig. 10B shows the same linear tendency between particle concentrations and PP concentrations as in Fig. 9A.

Parameter Correlations

Pearson's correlation coefficient for parameter relationships is shown in Table 4. The correlation between first-flush particle mass and first-flush PP mass (r = 0.66) agrees with the graph in Fig. 9B; first-flush colloid-facilitated transport obviously plays an important role in the leaching of phosphorus. The correlation between tritium recovery percentages and 5% arrival time is also high (r = −0.74). Fast 5% arrival time and high tritium recovery suggest highly preferential transport pathways and limited solute exchange with the inner soil matrix.

Bulk density is positively correlated with tritium recovery (r = 0.72) and negatively correlated with 5% arrival time (r = −0.68, Table 4, Fig. 11). This can be explained by a highly compacted soil with a high-bulk density having relatively few, but very continuous macropores, which can lead to preferential transport pathways with limited matrix transport, high tritium recoveries and fast 5% arrival times. In a less-compacted soil, water and solutes are exchanged between the main transport pathways and the inner, immobile soil matrix. This exchange retards solutes and leaves enough time for sorption and degradation limiting the amount of contaminants that reach underlying waters.

Assessing Field-Scale Vulnerability Zones

Our hypothesis is that a compacted, high-bulk density soil in the northern part of the field can lead to a low-permeable soil matrix with a decreased volumetric content of macropores. Yet, these macropores will likely be better aligned and connected, making the difference in hydraulic conductivity between macropores and soil matrix large enough to cause the onset of preferential flow events at lower rain intensities than for the less compacted soil at the southern part of the field. According to Jarvis et al. (2009), this phenomenon is characteristic for soils with relatively high clay contents, where the soils are often well structured with a system of macropores and relatively low hydraulic conductivity in the matrix. The Silstrup field has been a no-till system for almost 2 yr., giving the soil time to establish a stable structure with intact, connected, and

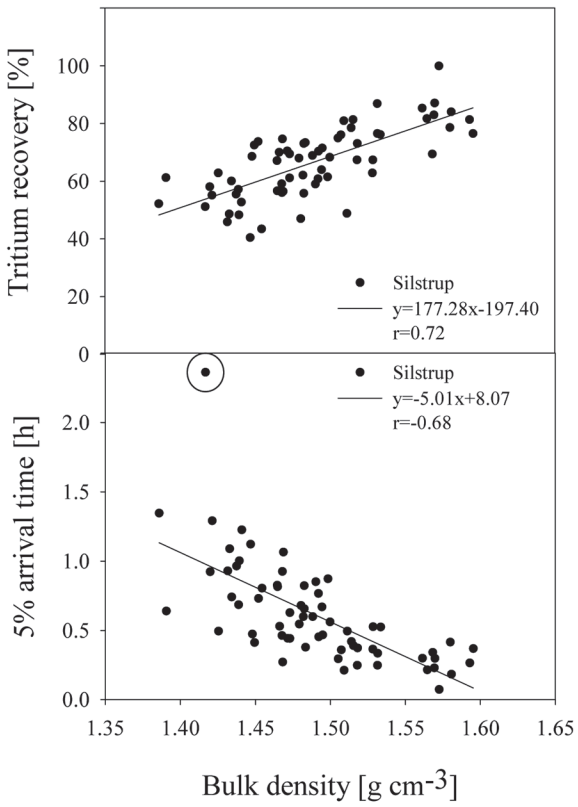

Fig. 11. Tritium recovery and 5% arrival time as a function of bulk density. In the lower figure column 73 has been circled. Without this point the regression would be: $y = -4.35x + 7.07$, $r^2 = -0.73$.

continuous macropores from the soil surface down through the soil profile. Activation of these macropores leads to an abrupt increase in the water flow rate by several orders of magnitude for only a small increase in soil water pressure (Iversen et al., 2011), and this will tend to promote particle and particle-facilitated transport as also indicated by the measurements. The amount of particulate matter leached through these macropores depends on whether there is a continuous supply of mobilized, stable particles in suspension. The supply of particles will be less from a no-till system as the one in Silstrup, as is also evident from the low first-flush particle concentrations compared with values from the literature. However, soil tillage will generate a large pool of easily mobilized particles that may contribute significantly to enhanced particle leaching through well-structured soils during rainstorm events. The map in Fig. 12 shows the total accumulated particle mass and PP mass leached at 60 mm outflow from the columns. According to this map, the largest mass of particles is leached from the northern part of the field (Fig. 12A). From Fig. 9 and similar literature studies by, for example, de Jonge et al. (2004b) and Schelde et al. (2006), we know that there is a strong positive correlation between the leaching of colloids and that of strongly sorbing compounds (Fig. 12B).

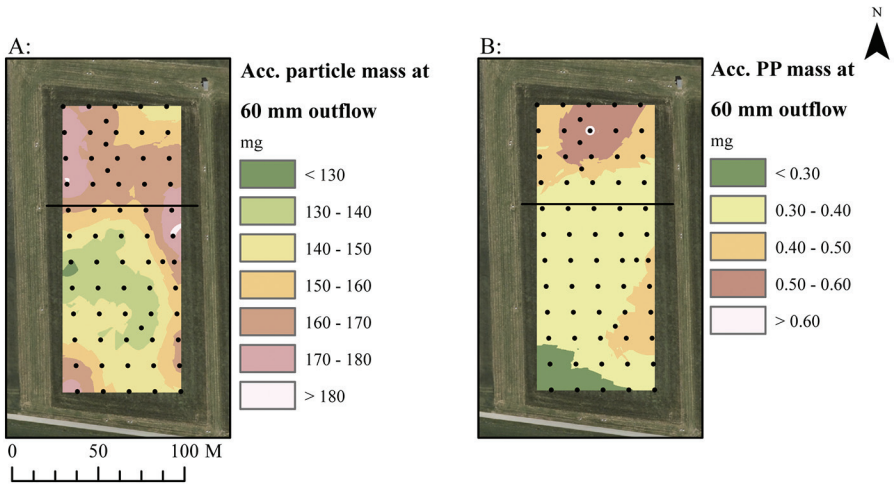

Fig. 12. Contour maps showing accumulated particle mass and particulate phosphorus (PP) mass leached at 60 mm outflow. The black intersecting lines delineate the upper one-third of the field.

The small-scale results achieved in this study were compared with field-scale monitoring results from Silstrup to see whether it is possible to predict field-scale vulnerability from small-scale measurements. Results from April 2000 through September 2009 from the Danish PLAP database have shown that there is a large difference in pesticide detections in water samples from the two horizontal wells H1 and H2 (Fig. 13, Fig. 1B). Pesticides were detected in 44% of the water samples from H1.2 (the middle screen section in the northern horizontal well, n = 115), whereas only 5% of the water samples from H2.2 (the middle screen section in the southern horizontal well, n = 113) contained detectable pesticide concentrations. The outer screen sections in H1 and H2 show the same remarkable dissimilarities. The reason for the different results is not entirely certain, but according to the theory presented in this study, the dissimilarities could be explained by differences in the soil physical structure across the field.

When assessing field-scale vulnerability zones some basic soil parameters (e.g., clay, silt, and OC content) are important. Soil structure also plays an important role, and the potential for particle release needs to be considered. In our study bulk density, tracer recovery and 5% tracer arrival time appeared to be promising indicators of soil structure. Because of our hypothesis about well-connected macropores in the northern part of the field, we expected air permeability and air-connected porosity to be high in this area of the field where we also detected fast 5% tracer arrival times and high tracer recoveries; however, this was not the case. Thus, air permeability and air-connected porosity at in situ conditions (Fig. 5A and B) were less promising as indicator parameters assessing field-scale vulnerability areas in this study. This seemingly disagrees with the findings by Loll et al. (1999) and Iversen et al. (2001) who found soil-air permeability measured on intact samples drained to −100 cm matric potential to well predict locations of high saturated hydraulic conductivity. This apparent disagreement is likely caused by the different drainage conditions applied. In this study the area in the southeastern part of the field with low bulk density (Fig. 3D) had well-connected pores for soil-air transport (Fig. 5A and B) under the given in situ conditions where the entire large-pore network was air-filled and likely participated in convective air transport. However, this did not directly translate to fast tracer and colloid transport at near-saturated conditions (Fig. 7 and Fig. 12) where the very largest pores (approximately > 300 microns diameter at the applied drainage of −20 cm matric potential) were not water-filled and, thus, not participating in the water, tracer, and colloid transport. Opposite, the high-bulk density areas in the northern

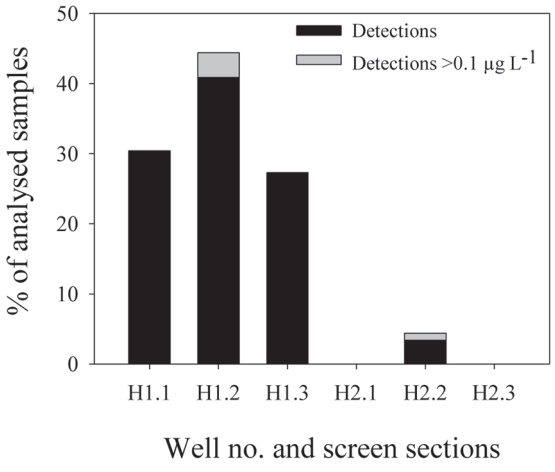

Fig. 13. Percentages of analyzed samples from the two horizontal wells (H1 to the north and H2 to the south, see Fig. 1B) containing one or more pesticides. Measured concentrations are either less than 0.1 µg L^{-1} (black) or above or equal to 0.1 µg L^{-1} (gray) in the period from April 6, 2000 through September 2009. Samples were collected monthly (H1.2 and H2.2, n = 113–115) or quarterly/half yearly (remaining filter sections, n = 20–24) (Kjær et al., 2011).

part of the field exhibited more straight and well-connected water-filled pores at near-saturation (−20 cm matric potential) and provided accelerated water, tracer, and colloid transport. In summary, it is essential to distinguish between near-saturated and fully fluid-saturated conditions when comparing and conveying measurements on intact soil columns to field-scale risk assessment.

Particle release can be estimated from basic soil texture, but Dexter's ratio, n, might be an even better indicator of soil stability and particle dispersibility. Schjønning et al. (2012) suggested a modified Dexter concept using a (clay + silt)/OC threshold ratio instead. The field in Silstrup was analyzed using only the original Dexter concept ($n \approx$ clay/OC), which seems promising for an initial zonation of this particular field. Nevertheless, a modified Dexter concept using both clay and silt can be a linking indicator/parameter that needs to be investigated further. Other parameters not considered in this study, for example the amount of water-dispersible colloids and tillage events, could also be used as indicators of particle release. However, the parameters presented in this paper were well able to characterize field-scale vulnerability zones within the field in Silstrup.

Conclusions

Particle concentrations and PP concentrations in the column effluent were positively correlated, indicating that the amount of water-dispersible colloids plays a role in the leaching of strongly sorbing compounds. This was further confirmed from the correlation between particle and PP concentrations measured on water samples from the shallow tile-drained system across the field in Silstrup.

Tracer parameters from leaching experiments were correlated to soil bulk density. The combination of highly compacted and clay-rich soil in the northern part of the field might lead to contaminant transport through preferential flow paths.

On the basis of soil physical parameters, bulk density and tracer parameters, it was possible to identify field-scale areas that, because of enhanced preferential transport, were vulnerable to leaching. A hitherto unexplainable long-term leaching phenomenon was determined to be caused by differences in soil physical structure. However, it is necessary to include dissolved chemical leaching parameters and colloid-associated leaching parameters in field-scale risk assessments in the future.

Acknowledgments

We thank S.T. Rasmussen, J.M. Nielsen, M. Koppelgaard, and P. Jørgensen for technical assistance in sampling and laboratory measurements. The study was funded by the international project Soil Infrastructure, Interfaces, and Translocation Processes in Inner Space (Soil-it-is) funded by the Danish Research Council for Technology and Production Sciences (http://www.agrsci.dk/soil-it-is/) and by the Danish Pesticide Leaching Assessment Programme (www.pesticidvarsling.dk).

References

Arnbjerg-Nielsen, K., Madsen, H., and Mikkelsen, P.S. 2006. Regional variation af ekstremregn i Danmark- ny bearbejdning (1979–2005), skrift 28. IDA Spildevandskomiteen, Denmark. http://ida.dk/netvaerk/fagtekniskenetvaerk/energimiljooguland/spildevandskomiteen/Documents/SVKskriftnr28.pdf (accessed 9 Oct. 2012).

Chen, C., and R.J. Wagenet. 1992. Simulation of water and chemicals in macropore soils.1. Representation of the equivalent macropore influence and its effect on soilwater flow. J. Hydrol. 130:105–126. doi:10.1016/0022-1694(92)90106-6

de Jonge, H., O.H. Jacobsen, L.W. de Jonge, and P. Moldrup. 1998. Particle-facilitated transport of prochloraz in undisturbed sandy loam soil columns. J. Environ. Qual. 27:1495–1503. doi:10.2134/jeq1998.00472425002700060028x

de Jonge, L.W., C. Kjaergaard, and P. Moldrup. 2004a. Colloids and colloid-facilitated transport of contaminants in soils: An introduction. Vadose Zone J. 3:321–325.

de Jonge, L.W., P. Moldrup, G.H. Rubaek, K. Schelde, and J. Djurhuus. 2004b. Particle leaching and particle-facilitated transport of phosphorus at field scale. Vadose Zone J. 3:462–470.

de Jonge, L.W., P. Moldrup, and P. Schjonning. 2009. Soil infrastructure, interfaces & translocation processes in inner space (Soil-it-is): Towards a road map for the constraints and crossroads of soil architecture and biophysical processes. Hydrol. Earth Syst. Sci. 13:1485–1502. doi:10.5194/hess-13-1485-2009

Dexter, A.R., G. Richard, D. Arrouays, E.A. Czyz, C. Jolivet, and O. Duval. 2008. Complexed organic matter controls soil physical properties. Geoderma 144:620–627. doi:10.1016/j.geoderma.2008.01.022

El-Farhan, Y.H., N.M. Denovio, J.S. Herman, and G.M. Hornberger. 2000. Mobilization and transport of soil particles during infiltration experiments in an agricultural field, Shenandoah Valley, Virginia. Environ. Sci. Technol. 34:3555–3559. doi:10.1021/es991099g

Etana, A., T. Rydberg, and J. Arvidsson. 2009. Readily dispersible clay and particle transport in five Swedish soils under long-term shallow tillage and mouldboard ploughing. Soil Tillage Res. 106:79–84. doi:10.1016/j.still.2009.09.016

Fox, G.A., R. Malone, G.J. Sabbagh, and K. Rojas. 2004. Interrelationship of macropores and subsurface drainage for conservative tracer and pesticide transport. J. Environ. Qual. 33:2281–2289. doi:10.2134/jeq2004.2281

Gee, G.W., and D. Or. 2002. Methods of soil analysis. Part 4. Physical methods. SSSA Book Ser. 5. SSSA, Madison, WI.

Geological Survey of Denmark and Greenland. 1999. Digitalt kort over Danmarks jordarter 1:200000; GEUS rapport 1999/47. (In Danish.) Geological Survey of Denmark and Greenland, Copenhagen, Denmark.

Geological Survey of Denmark and Greenland. 2009. Grundvandsovervågningen 2009—Grundvand. Status og udvikling 1989–2008. De Nationale og Geologiske Undersøgelser for Danmark og Grønland, Klima-og Energiministeriet, Copenhagen, Denmark.

Gjettermann, B., C.T. Petersen, C.B. Koch, N.H. Spliid, C. Gron, D.L. Baun, and M. Styczen. 2009. Particle-facilitated pesticide leaching from differently structured soil monoliths. J. Environ. Qual. 38:2382–2393. doi:10.2134/jeq2008.0417

Glaesner, N., C. Kjaergaard, G.H. Rubaek, and J. Magid. 2011. Interactions between soil texture and placement of dairy slurry application: I. Flow characteristics and leaching of nonreactive components. J. Environ. Qual. 40:337–343. doi:10.2134/jeq2010.0317

Grant, R., A. Laubel, B. Kronvang, H.E. Andersen, L.M. Svendsen, and A. Fuglsang. 1996. Loss of dissolved and particulate phosphorus from arable catchments by subsurface drainage. Water Res. 30:2633–2642. doi:10.1016/S0043-1354(96)00164-9

Iversen, B.V., C.D. Borgesen, M. Laegdsmand, M.H. Greve, G. Heckrath, and C. Kjaergaard. 2011. Risk predicting of macropore flow using pedotransfer functions, textural maps, and modeling. Vadose Zone J. 10:1185–1195. doi:10.2136/vzj2010.0140

Iversen, B.V., P. Moldrup, P. Schjonning, and P. Loll. 2001. Air and water permeability in differently textured soils at two measurement scales. Soil Sci. 166:643–659. doi:10.1097/00010694-200110000-00001

Jacobsen, O.H., and J. Kjaer. 2007. Is tile drainage water representative of root zone leaching of pesticides? Pest Manage. Sci. 63:417–428. doi:10.1002/ps.1372

Jarvis, N.J. 2007. A review of non-equilibrium water flow and solute transport in soil macropores: Principles, controlling factors and consequences for water quality. Eur. J. Soil Sci. 58:523–546. doi:10.1111/j.1365-2389.2007.00915.x

Jarvis, N., M. Larsbo, S. Roulier, A. Lindahl, and L. Persson. 2007. The role of soil properties in regulating non-equilibrium macropore flow and solute transport in agricultural topsoils. Eur. J. Soil Sci. 58:282–292. doi:10.1111/j.1365-2389.2006.00837.x

Jarvis, N.J., J. Moeys, J.M. Hollis, S. Reichenberger, A.M.L. Lindahl, and I.G. Dubus. 2009. A conceptual model of soil susceptibility to macropore flow. Vadose Zone J. 8:902–910. doi:10.2136/vzj2008.0137

Keller, T., and I. Hakansson. 2010. Estimation of reference bulk density from soil particle size distribution and soil organic matter content. Geoderma 154:398–406. doi:10.1016/j.geoderma.2009.11.013

Kjaer, J., V. Ernsten, O.H. Jacobsen, N. Hansen, L.W. de Jonge, and P. Olsen. 2011. Transport modes and pathways of the strongly sorbing pesticides glyphosate and pendimethalin through structured drained soils. Chemosphere 84:471–479. doi:10.1016/j.chemosphere.2011.03.029

Kjaer, J., P. Olsen, K. Bach, H.C. Barlebo, F. Ingerslev, M. Hansen, and B.H. Sorensen. 2007. Leaching of estrogenic hormones from manure-treated structured soils. Environ. Sci. Technol. 41:3911–3917. doi:10.1021/es0627747

Kjær, J., A.E. Rosenbom, W. Brüsch, R.K. Juhler, L. Gudmundsson, F. Plauborg, R. Grant, and P. Olsen. 2011. The Danish Pesticide Leaching Assessment Programme: Monitoring results May 1999–June 2010. Geological Survey of Denmark and Greenland, Copenhagen, Denmark.

Kjaergaard, C., T.G. Poulsen, P. Moldrup, and L.W. de Jonge. 2004. Colloid mobilization and transport in undisturbed soil columns. I. Pore structure characterization and tritium transport. Vadose Zone J. 3:413–423.

Koestel, J.K., J. Moeys, and N.J. Jarvis. 2011. Evaluation of nonparametric shape measures for solute breakthrough curves. Vadose Zone J. 10:1261–1275. doi:10.2136/vzj2011.0010

Koroleff, F. 1983. Simultaneous oxidation of nitrogen and phosphorus compounds by persulfate. In: K. Grasshoff, M. Eberhardt, and K. Kremling, editors, Methods of seawater analysis. Verlag Chemie, Weinheimer, Germany. p. 168–169.

Laubel, A., O.H. Jacobsen, B. Kronvang, R. Grant, and H.E. Andersen. 1999. Subsurface drainage loss of particles and phosphorus from field plot experiments and a tile-drained catchment. J. Environ. Qual. 28:576–584. doi:10.2134/jeq1999.00472425002800020023x

Lindhardt, B., C. Abildtrup, H. Vosgerau, P. Olsen, S. Torp, B.V. Iversen, J.O. Jørgensen, F. Plauborg, P. Rasmussen, and P. Gravesen. 2001. The Danish Pesticide Leaching Assessment Programme: Site characterization and monitoring design. Geological Survey of Denmark and Greenland, Copenhagen, Denmark.

Loll, P., P. Moldrup, P. Schjonning, and H. Riley. 1999. Predicting saturated hydraulic conductivity from air permeability: Application in stochastic water infiltration modeling. Water Resour. Res. 35:2387–2400. doi:10.1029/1999WR900137

Majdalani, S., E. Michel, L. Di-Pietro, and R. Angulo-Jaramillo. 2008. Effects of wetting and drying cycles on in situ soil particle mobilization. Eur. J. Soil Sci. 59:147–155. doi:10.1111/j.1365-2389.2007.00964.x

McCarthy, J.F., L.D. Mckay, and D.D. Bruner. 2002. Influence of ionic strength and cation charge on transport of colloidal particles in fractured shale saprolite. Environ. Sci. Technol. 36:3735–3743. doi:10.1021/es025522o

Murphy, J., and J.P. Riley. 1962. A modified single solution method for determination of phosphate in natural waters. Anal. Chim. Acta 27:31–36. doi:10.1016/S0003-2670(00)88444-5

National Environmental Research Institute. 2000. Areal Informations Systemet (AIS). (In Danish.) National Environmental Research Institute, Denmark.

Poulsen, T.G., P. Moldrup, L.W. de Jonge, and T. Komatsu. 2006. Colloid and bromide transport in undisturbed soil columns: Application of two-region model. Vadose Zone J. 5:649–656. doi:10.2136/vzj2005.0068

Schelde, K., L.W. de Jonge, C. Kjaergaard, M. Laegdsmand, and G.H. Rubaek. 2006. Effects of manure application and plowing on transport of colloids and phosphorus to tile drains. Vadose Zone J. 5:445–458. doi:10.2136/vzj2005.0051

Schelde, K., P. Moldrup, O.H. Jacobsen, H. de Jonge, L.W. de Jonge, and T. Komatsu. 2002. Diffusion-limited mobilization and transport of natural colloids in macroporous soil. Vadose Zone J. 1:125–136.

Schjønning, P., L.W. de Jonge, L.J. Munkholm, P. Moldrup, B.T. Christensen, and J.E. Olesen. 2012. Clay dispersibility and soil friability: Testing the soil clay-to-carbon saturation concept. Vadose Zone J. 11(1). doi:10.2136/vzj2011.0067

Vendelboe, A.L., P. Moldrup, G. Heckrath, Y. Jin, and L.W. de Jonge. 2011. Colloid and phosphorus leaching from undisturbed soil cores sampled along a natural clay gradient. Soil Sci. 176:399–406. doi:10.1097/SS.0b013e31822391bc

Villholth, K.G., N.J. Jarvis, O.H. Jacobsen, and H. de Jonge. 2000. Field investigations and modeling of particle-facilitated pesticide transport in macroporous soil. J. Environ. Qual. 29:1298–1309. doi:10.2134/jeq2000.00472425002900040037x